CHINESE OPTICS LETTERS

Vol. 19, No. 10 | October 2021

Polarization dependent clamping intensity inside a femtosecond filament in air

Hao Guo (郭 豪)[1,2], Xiang Dong (董 翔)[3], Tie-Jun Wang (王铁军)[1,2*], Xuan Zhang (张 旋)[1], Na Chen (陈 娜)[1], Fukang Yin (尹富康)[1,2], Yihai Wang (王依海)[1,4], Lingang Zhang (张临港)[1], Haiyi Sun (孙海轶)[1], Jun Liu (刘 军)[1,2], Jiansheng Liu (刘建胜)[5], Baifei Shen (沈百飞)[5], Olga Kosareva[6], Yuxin Leng (冷雨欣)[1,2], and Ruxin Li (李儒新)[1,2]

[1] State Key Laboratory of High Field Laser Physics and CAS Center for Excellence in Ultra-intense Laser Science, Shanghai Institute of Optics and Fine Mechanics, Chinese Academy of Sciences, Shanghai 201800, China

[2] Center of Materials Science and Optoelectronics Engineering, University of Chinese Academy of Sciences, Beijing 100049, China

[3] Department of Physics, College of Arts and Science, University of Colorado Boulder, Boulder, CO 80309, USA

[4] College of Physics, Guizhou University, Guiyang 550025, China

[5] Department of Physics, Shanghai Normal University, Shanghai 200234, China

[6] Physics Faculty, Lomonosov Moscow State University, Moscow 119991, Russia

*Corresponding author: tiejunwang@siom.ac.cn

Received February 6, 2021 | Accepted March 18, 2021 | Posted Online August 9, 2021

Laser polarization and its intensity inside a filament core play an important role in filament-based applications. However, polarization dependent clamping intensity inside filaments has been overlooked to interpret the polarization-related filamentation phenomena. Here, we report on experimental and numerical investigations of polarization dependent clamping intensity inside a femtosecond filament in air. By adjusting the initial polarization from linear to circular, the clamping intensity is increased by 1.36 times when using a 30 cm focal length lens for filamentation. The results indicate that clamping intensity inside the filament is sensitive to laser polarization, which has to be considered to fully understand polarization-related phenomena.

Keywords: femtosecond laser filamentation; clamping intensity; polarization.
DOI: 10.3788/COL202119.103201

1. Introduction

Recently, there has been an ascending interest in a large variety of promising applications of femtosecond (fs) laser filamentation[1–8] ranging from supercontinuum generation[1,9,10], terahertz (THz) radiation[3,4], air lasing[11,12], and guiding corona discharges[13,14] to driving ionic wind[15]. Initial laser polarization plays an important and critical role in filament-based applications. There are several phenomena observed under specific laser polarization states for filamentation. For instance, the circularly polarized beam less effectively induced multiple filaments[16], strong backward stimulated radiation was observed from neutral nitrogen at 337 nm only under circular polarization (CP)[17], and the efficiency of THz emission from two-color filamentation was significantly enhanced under the circularly polarized laser compared with the linearly polarized one[18]. Besides, filament-induced supercontinuum generation is found to be highly dependent on the initial laser polarization[10,19,20]. Few numerical simulations have been made to predict the laser polarization-related filamentation process[21–23]. Kolesik *et al.*[23] theoretically reported that the circularly polarized pulses created lower plasma densities compared to the linearly polarized pulses. Panov and co-workers' simulation[22] indicated a higher clamping intensity under CP than under linear polarization (LP). In 2013, the same group developed a theoretical model of fs filamentation[21], which included the high-order Kerr effect, instead ignoring the effect of plasma. Their simulation results showed that when laser polarization was adjusted from LP to CP, the maximum filament intensity had a step-like increase. Recently, by tuning laser polarization, the control of fs filamentation has been well demonstrated experimentally[24].

The physical picture of the polarization dependence on the filamentation behavior has not been fully disclosed. One general interpretation is the influence on the accelerating process of the free electron driven by the different polarizations[25,26]. With a linearly polarized laser, free electrons are left with low kinetic energies (~ 1 eV) due to the alternative acceleration and deceleration in each optical cycle of the laser field. In contrast, with a circularly polarized laser, electrons are always accelerated away

from the molecular ion. Therefore, an almost monoenergetic distribution around 14.6 eV is achieved for circular laser polarization[26]. Apparently, the effect of initial polarization on laser intensity (or strength of the laser electric field) inside the filament is overlooked. The direct measurement of polarization dependent laser intensities inside a filament would benefit the understanding of the laser polarization sensitive phenomenon, which is still absent so far.

Experimental measurement of filament intensity is nontrivial due to the onset of material damage on components placed in the beam path. Therefore, the intensity of the filament is generally obtained through indirect approaches[27–29]. Recently, Liu *et al.*[30] directly measured the fluence profiles in fs laser filaments in air based on the incidence angle dependence of the single-shot laser ablation threshold on the gold sample. Mitryukovskiy *et al.*[31] reported on a direct measurement method of "burning hole". By inserting a metallic foil inside a filament, the laser filament will drill a pinhole with a diameter of the filament. Then, the intensity inside the filament was obtained from the trivial measurements of filtered out pulse energy and the duration of the filament pulse. Following the method, Li *et al.*[32] successfully measured the clamping intensity inside a filament in a flame. More recently, the modulation of the radial fluence profiles inside a filament core was directly measured by using the "burning hole" method[33].

In this Letter, we present an experimental study of the polarization dependence on laser intensity inside an air filament by employing the "burning hole" approach. In addition, numerical simulations based on the extended nonlinear Schrödinger equation (NLSE) are performed to support the experimental observations. The results in the work indicate that filament intensity is sensitive to the initial laser polarization, which has to be considered in order to fully understand the polarization sensitive phenomena of the filament applications.

2. Experimental Methods and Results

The experimental setup is shown in Fig. 1. The input laser pulses were generated from a Ti:sapphire chirped pulse amplification (CPA) laser system with a central wavelength of 800 nm, 20 Hz repetition rate, and 32 fs pulse duration. A stellate aperture with a diameter of 6 mm was used to get rid of the initial diffraction on the laser pulse and obtain an input laser beam with a clean Gaussian profile[33]. The initial laser with LP was adjusted by a quarter-wave plate (QWP) to provide different initial ellipticities. A mechanical shutter was employed to control the laser pulse numbers passing through it. The input laser beam was focused by plano-convex lenses with a 30 cm or 100 cm focal length, respectively. Since laser intensity is clamped inside the filament even with the increase of laser energy[8], the laser pulse energy used in the experiment ranges from a few hundred microjoules (μJ) to about 1.8 mJ with emphasis at the single filament region. The filament "burning hole" technique on aluminum (Al) foils with uniform thickness of approximately 15 μm was employed to measure filament intensity[31]. The areas of filament-drilled pinholes were evaluated by a transmission microscope. The transmitted filament energy and pulse duration after the filament-drilled pinhole were recorded by an energy meter (Coherent FieldMaxII) and an autocorrelator (APE PulseCheck), respectively.

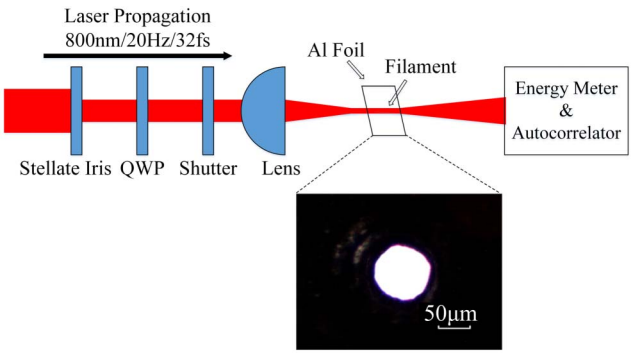

Fig. 1. Experimental setup. The inset shows a typical picture of a filament-drilled pinhole.

Figure 2(a) shows the side fluorescence images of the LP and CP filaments with an $f = 30$ cm lens. The images taken by a digital camera were accumulated for 40 shots. The 1/e lengths of the LP and CP filaments are 9.44 mm and 9.40 mm, respectively. As shown in Fig. 2(b), under the condition of 1 mJ /LP/$f = 30$ cm, the filament-drilled pinhole's diameter changes as a function of the input laser pulse number due to the accumulation effect[31]. The Al foils were placed at the most intense position of filament. The pinhole diameter gradually rises from approximately 60 μm after 20 shots to a stable value of approximately 100 μm after 120 shots, which agrees with the experimental observation in other works at similar conditions[7]. The energy reservoir of the filament is not intense enough to break the metallic foil even if the shot number is comparatively large.

To obtain the fluence distribution along the filaments, a group of pinholes (approximately 42.3 μm in radius) were prepared under the condition of 300 shots/1 mJ/32 fs/LP. After that, a single shot of filament with 1 mJ energy was released to pass through the pinholes. The pinholes were used to sample out the energy at different longitudinal positions along the filament core. Laser fluences at different positions could be experimentally obtained through Fluence$(z) = E(z)/S(z)$, where $E(z)$ and $S(z)$ are the transmitted laser energy and the pinhole area at the position z, respectively. Each pinhole was used only once. The measurement at each position along the filaments was repeated five times. It is noted that all of the pinholes were made with the same linearly polarized filaments. These pinholes were then used for intensity measurements of filaments under different laser polarizations. The experimental results are shown in Fig. 2(c), which are fitted by the polynomial fitting as a guide for the eye. It is clearly shown that laser fluence of a circularly polarized filament is higher than that of the linearly polarized one.

At the most intense position along filaments [maximum fluence position shown in Fig. 2(c)], the input pulse energy dependent laser fluence inside the filament core (with a diameter of

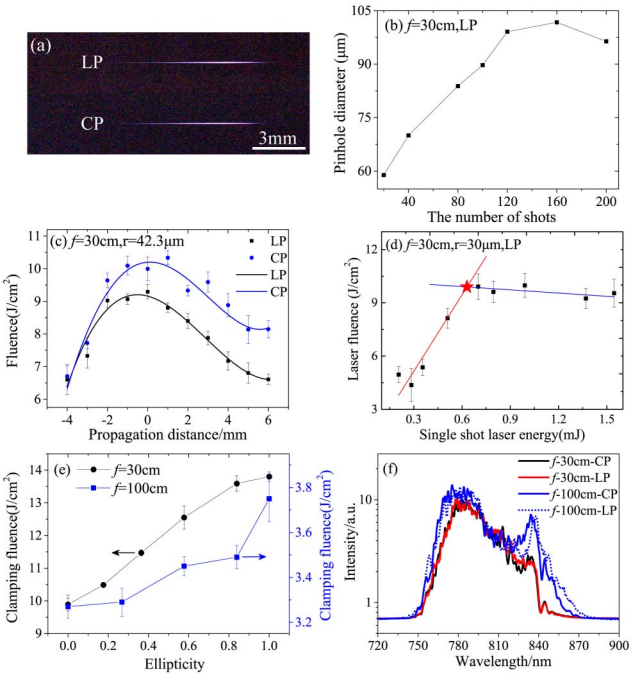

Fig. 2. (a) Side fluorescence images of filaments in LP and CP with $f = 30$ cm focusing lens. The images were accumulated for 40 shots. (b) The diameters of the laser filament-drilled ($f = 30$ cm) Al foil pinholes as a function of the number of the laser shots. The laser energy was 1 mJ. (c) Measured laser fluence distribution along the LP or CP filaments ($f = 30$ cm). The solid curves are polynomial fits as a guide for the eye. The radius of the pinhole was approximately 42.3 μm. The position "0" corresponds to the geometry focus ($f = 30$ cm), while the positive values indicate the positions prior to the geometry focus. (d) Measured laser fluence with $f = 30$ cm focusing lens as a function of the input laser energy at LP (ellipticity of zero). (e) Clamping laser fluence inside the filament core versus different initial laser polarization ellipticities under the external focusing conditions of $f = 30$ cm and $f = 100$ cm, respectively. (f) Laser spectra measured after filamentation.

60 μm corresponding to ~FWHM filament diameter of 100 μm) was measured using filament prepared pinholes. The result is shown in Fig. 2(d). The initial ellipticity was set as zero (LP), and an $f = 30$ cm lens was used. With increasing laser energy, the laser fluence first grows linearly and then stays almost at a constant value, which is in good agreement with Ref. [31]. The red star at (9.89 J/cm^2, 0.63 mJ) in Fig. 2(d) marks the intersection points of these two regimes. The fluence at this intersection point is equal to the clamping fluence of the LP filament[31–33]. Furthermore, the polarization dependence on the clamping fluence was measured according to the different intersection data, as presented in Fig. 2(e). With the initial ellipticity adjusting from 1 to 0, as polarization changes from CP to LP, the laser clamping fluence inside the filament core decreases from 13.80 ± 0.14 to 9.89 ± 0.19 J/cm^2. The ratio of laser clamping fluence evaluated at the initial CP to LP is approximately 1.4. Compared with Fig. 2(e), the diameter of the pinholes used in Fig. 2(c) is larger; therefore, the measured laser fluence is a little lower in Fig. 2(c).

To investigate the impact of external focusing conditions on the clamping laser fluence, another set of experiments was carried out with a 100 cm focal length plano-convex lens. The same procedure was performed under 100 cm focusing condition to drill the pinholes using the laser filament first and to measure the laser fluence inside the filament core at the FWHM diameter. The measured clamping fluences are shown in Fig. 2(e) with a blue line and a blue square. The clamping fluence obtained with $f = 100$ cm was lower than that of the $f = 30$ cm case because of the external geometrical focusing effect[34]. Similar dependence of clamping fluence on laser ellipticity is observed. By adjusting the initial ellipticity from 1 to 0, the laser fluence inside the filament core decreases from 3.75 ± 0.10 to 3.27 ± 0.05 J/cm^2. The ratio of laser fluence evaluated at the initial CP to LP is approximately 1.2.

In order to obtain the laser intensity inside the filament, the pulse duration after filamentation was obtained by the autocorrelator. The output laser pulse duration was 32 fs at FWHM. However, after 6 m propagation in air, from the laser system to the experimental table, and after propagation through several mirrors, neutral density filters, and the QWP, the pulse duration before the focusing lens was measured to be 70 fs, which indicated that the initial laser pulse for filamentation had some positive chirp. In the case of $f = 30$ cm, the retrieved pulse durations of the initial CP and LP pulses after filamentation were stretched to 73 fs and 71 fs, respectively. The spectra measured after filamentation are almost the same [black and red lines in Fig. 2(f)]. According to the pulse durations obtained, the measured peak laser intensity inside filament core is $(18.90 \pm 0.19) \times 10^{13}$ W/cm^2 for the input CP laser. For LP, the intensity is approximately $(13.93 \pm 0.27) \times 10^{13}$ W/cm^2, which is 1.36 times smaller than that of the CP one. In the case of $f = 100$ cm, the FWHMs of the laser spectra obtained with the LP laser are slightly wider than those of the CP laser, because the self-phase modulation effect is more significant in the LP laser filamentation[20]. The pulse durations after filamentation are measured to be 111 fs and 113 fs for the LP and CP lasers, respectively. Therefore, laser intensities inside LP and CP laser filaments are $(3.32 \pm 0.09) \times 10^{13}$ W/cm^2 and $(2.95 \pm 0.04) \times 10^{13}$ W/cm^2, respectively. The intensity ratio of the CP and LP filaments is approximately 1.12. Compared with the $f = 30$ cm case, the pulse durations measured in the $f = 100$ cm case are broader, which may be attributed to more positive chirp from the pronounced self-phase modulation effect and less negative chirp from the plasma effect[35]. Therefore, additional positive chirp should be generated for the filament by the $f = 100$ cm lens, which may be the reason for the pulse broadening.

3. Numerical Results

The polarization dependent clamping intensity phenomenon is also numerically investigated by solving the extended NLSE[36]. Assuming an axially symmetrical laser beam with a Gaussian profile in both time and space domains, which propagates along the z axis, the input laser beam can be depicted as[37]

$$\varepsilon^{\pm}(r,t,z=0)=[(1\pm\theta)/2]^{1/2}A_0\exp\left(-\frac{r^2}{2r_0^2}-\frac{t^2}{2t_p^2}-i\frac{kr^2}{2f}\right). \quad (1)$$

To account for arbitrary polarization, the electric field is decomposed into a linear combination of left- and right-hand circular components $\varepsilon^{\pm}=\frac{E_x\pm iE_y}{\sqrt{2}}$[21]. A_0 is the amplitude of the incident laser field, $r_0=1.64$ mm is the waist of the initial beam (1/e), $f=30$ cm, 50 cm, and 100 cm are the lens focal lengths, and $t_p=32$ fs is the pulse duration. θ is the laser ellipticity, where $\theta=0$ and 1 indicate that the input laser polarizations are LP and CP, respectively.

The nonlinear propagation process can be described as[23,38,39]

$$\frac{\partial\varepsilon^{\pm}}{\partial z}=\frac{i}{2k}\nabla_{\perp}^2\varepsilon^{\pm}-\frac{ik''}{2}\frac{\partial^2\varepsilon^{\pm}}{\partial t^2}+i\frac{2\omega}{3c}n_2(|\varepsilon^{\pm}|^2+2|\varepsilon^{\mp}|^2)\varepsilon^{\pm}-\frac{1}{2}\frac{(\rho_O W_O K_O+\rho_N W_N K_N)\hbar\omega}{I}\varepsilon^{\pm}-\frac{\sigma}{2}(1+i\omega t)\rho\varepsilon^{\pm}. \quad (2)$$

The values of the parameters used in Eq. (2) were taken from Refs. [21,36–39]. To complete the simulation, the evolution equations of the densities of oxygen (ρ_O) and nitrogen (ρ_N) are expressed as[39]

$$\frac{\partial\rho_N}{\partial t}=-W_N\rho_N$$
$$\frac{\partial\rho_O}{\partial t}=-W_O\rho_O. \quad (3)$$

The LP and CP laser ionization rates (W_N and W_O) are calculated according to Perelomov, Popov, and Terent'ev's model (PPT model)[40] with Coulomb correction[41]. Then, the elliptically polarized laser ionization rates are calculated by performing a quadratic interpolation between the LP and CP laser ionization rates[38].

In the simulations, the input laser energies were kept at $E_{in}=1$ mJ. The intensity values in Fig. 3 are obtained as follows: first, the original intensity values are averaged in the range of $r<30$ μm, 30 μm, and 39 μm (the radii of the pinholes) in the case of $f=30$ cm, 50 cm, and 100 cm, respectively. Then, the maximum of the intensity values in the time domain at each propagation position is retrieved. The simulated maximum intensity of the CP filament is higher than that of the LP one [Fig. 3(a)], which is in consistent with the measurement [Fig. 2(c)]. The laser intensity increases with a relatively smaller slope in the LP case. The simulated peak intensity in the CP filament (11.30×10^{13} W/cm^2) is 1.35 times higher than that in the LP filament (8.37×10^{13} W/cm^2), which is very close to the experimental results of 1.36. Compared with experimental results, the intensities obtained in the simulations are slightly lower, which may be attributed to the fact that the spatial profile of the initial laser intensity is not ideally Gaussian[33]. Furthermore, Fig. 3(a) also demonstrates that the peak intensity has negligible change when increasing the input laser energy to 1.7 mJ for LP filamentation. Moreover, when the initial pulse duration is stretched to 70 fs, the intensity ratio of CP and LP

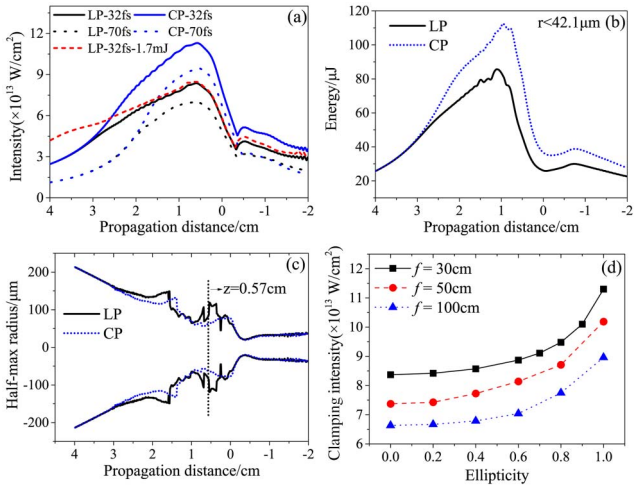

Fig. 3. (a) Peak intensity as a function of propagation distances. The focal length is 30 cm unless it is stated. (b) Laser energy confined in the range of $r<42.1$ μm as a function of propagation distance. (c) The beam sizes (fluence at FWHM) as a function of propagation distances. The vertical dot line indicates the propagation distance ($z=0.57$ cm), where the maximum intensity during the propagation is obtained in the CP case. In the LP case, the maximum intensity is obtained at $z=0.59$ cm. (d) Simulated clamping intensity versus the initial laser polarization ellipticity under external focusing conditions of $f=30$ cm, 50 cm, and 100 cm, respectively.

is also approximately 1.35, which indicates that the intensity ratio is independent on the initial pulse duration.

The evolution of laser energy confined in the range of $r<42.1$ μm [close to the pinhole radius in Fig. 2(c)] and the beam radius at FWHM are shown in Figs. 3(b)–3(c), respectively. It is clear that less laser energy is confined in the range of $r<42.1$ μm in the LP case, and the beam radius of the LP filament is larger than that in the CP case. The simulated clamping intensities (defined as the peak intensities obtained during the propagation) inside filaments as a function of ellipticity are shown in Fig. 3(d) under different focusing conditions. By adjusting laser polarization from LP to CP, the clamping intensities gradually increase for all of the cases. Compared with the simulation results in Ref. [21], no intensity jump at a specific ellipticity region is observed in our simulation. The ratios of the peak intensity between CP and LP are 1.38 and 1.35 for $f=50$ cm and $f=100$ cm, respectively. The simulated intensity ratio under the $f=100$ cm focusing condition is higher than the experimentally determined ratio of 1.12. The difference may be attributed to the fact that the pulse duration is measured at the end of the filament, which may deviate from the simulated pulse duration at a specific propagation position inside the filament.

The higher peak intensity in the CP filament can be attributed to the polarization dependent ionization process: compared with the CP laser, the LP laser has a higher ionization rate[42], therefore, the LP laser-induced plasma should be denser, and the laser beam should experience a stronger defocusing effect. This is evidenced by Figs. 3(a)–3(c). Besides, the critical power for

self-focusing, $P_{cr} = 3.72\lambda^2/8\pi n_0 n_2$, is inversely proportional to the nonlinear index coefficient, n_2, at a given wavelength. Since the n_2 for the LP pulse is 1.5 times the n_2 for the CP pulse[43], the P_{cr} of the CP laser is 1.5 times that of the LP laser, which leads to earlier self-focusing for the LP pulse compared with the CP pulse. The assumption is verified both in the experiment[24] and in the simulation. For example, at the early stage of propagation (at $z = 4$ cm), the laser beam exhibits a peak power of 24.9 GW, which is approximately 8.3 times the P_{cr} (LP) and 5.5 times the P_{cr} (CP). Thus, the onset position of the CP pulse filament is delayed (closer to the geometrical focus) compared with the LP laser filament. As a consequence, more laser energy should be confined in the vicinity of the optical axis through geometrical focusing, which is confirmed in our experiments. However, as shown in the simulation (Fig. 3), laser filamentation is a highly complicated nonlinear process. The polarization dependent n_2 as well as P_{cr} alone cannot fully explain the polarization dependent clamping intensity phenomenon.

4. Conclusion

We systematically investigate the input laser polarization effect on the clamping intensity inside an air filament. Through a simple method of the filament burning holes on Al foils, the laser polarization dependent clamping intensity inside a filament was directly measured in air. As the incident laser is circularly polarized for filamentation, the measured laser intensity clamped inside the filament is 1.36 times ($f = 30$ cm) higher than the one induced by the linearly polarized laser. The clamping intensity gradually decreases when the input laser polarization is tuned from CP to LP. Simulations based on the extended NLSE are performed to support the experimental observation. The results in this work clarify the disputes on the prediction of filament clamping intensity both experimentally and numerically[21–23]. Although the experiments and simulations are performed in air, the results may apply for other filamentation media. The polarization sensitive clamping intensity results inside a filament have to be considered towards understanding the mechanisms of the polarization dependent phenomena observed[16–19].

Acknowledgement

This work was supported in part by the Strategic Priority Research Program of the Chinese Academy of Sciences (No. XDB16010400) and the International Partnership Program of Chinese Academy of Sciences (Nos. 181231KYSB20160045 and 181231KYSB20200033). Olga Kosareva acknowledges the support from the Russian Science Foundation (No. 21-49-00023).

Reference

1. J. Kasparian and J. P. Wolf, "Physics and applications of atmospheric nonlinear optics and filamentation," Opt. Express **16**, 466 (2008).
2. J. P. Wolf, "Short-pulse lasers for weather control," Rep. Prog. Phys. **81**, 026001 (2018).
3. S. L. Chin, T. J. Wang, C. Marceau, J. Wu, J. S. Liu, O. Kosareva, N. Panov, Y. P. Chen, J. F. Daigle, S. Yuan, A. Azarm, W. W. Liu, T. Seideman, H. P. Zeng, M. Richardson, R. Li, and Z. Z. Xu, "Advances in intense femtosecond laser filamentation in air," Laser Phys. **22**, 1 (2012).
4. V. P. Kandidov, S. A. Shlenov, and O. G. Kosareva, "Filamentation of high-power femtosecond laser radiation," Quantum Electron. **39**, 205 (2009).
5. L. Berge, S. Skupin, R. Nuter, J. Kasparian, and J. P. Wolf, "Ultrashort filaments of light in weakly ionized, optically transparent media," Rep. Prog. Phys. **70**, 1633 (2007).
6. A. Couairon and A. Mysyrowicz, "Femtosecond filamentation in transparent media," Phys. Rep. **441**, 47 (2007).
7. S. L. Chin, S. A. Hosseini, W. Liu, Q. Luo, F. Theberge, N. Akozbek, A. Becker, V. P. Kandidov, O. G. Kosareva, and H. Schroeder, "The propagation of powerful femtosecond laser pulses in optical media: physics, applications, and new challenges," Can. J. Phys. **83**, 863 (2005).
8. S. L. Chin, *Femtosecond Laser Filamentation* (Springer, 2010).
9. S. L. Chin, A. Brodeur, S. Petit, O. G. Kosareva, and V. P. Kandidov, "Filamentation and supercontinuum generation during the propagation of powerful ultrashort laser pulses in optical media (white light laser)," J. Nonlinear Opt. Phys. Mater. **8**, 121 (1999).
10. Y. Liu, T.-J. Wang, N. Chen, H. Guo, H. Sun, L. Zhang, Z. Qi, Y. Leng, Z. Wang, and R. Li, "Simultaneous generation of controllable double white light lasers by focusing an intense femtosecond laser pulse in air," Chin. Opt. Lett. **18**, 121402 (2020).
11. Q. Luo, W. Liu, and S. L. Chin, "Lasing action in air induced by ultra-fast laser filamentation," Appl. Phys. B **76**, 337 (2003).
12. J. P. Yao, B. Zeng, H. L. Xu, G. H. Li, W. Chu, J. L. Ni, H. S. Zhang, S. L. Chin, Y. Cheng, and Z. Z. Xu, "High-brightness switchable multiwavelength remote laser in air," Phys. Rev. A **84**, 051802 (2011).
13. Y. X. Liu, T. J. Wang, N. Chen, S. Z. Du, J. J. Ju, H. Y. Sun, C. Wang, J. S. Liu, H. H. Lu, S. L. Chin, R. X. Li, Z. Z. Xu, and Z. S. Wang, "Probing the effective length of plasma inside a filament," Opt. Express **25**, 11078 (2017).
14. T. J. Wang, Y. X. Wei, Y. X. Liu, N. Chen, Y. H. Liu, J. J. Ju, H. Y. Sun, C. Wang, H. H. Lu, J. S. Liu, S. L. Chin, R. X. Li, and Z. Z. Xu, "Direct observation of laser guided corona discharges," Sci. Rep. **5**, 18681 (2016).
15. S. Z. Du, T. J. Wang, Z. B. Zhu, Y. X. Liu, N. Chen, J. H. Zhang, H. Guo, H. Y. Sun, J. J. Ju, C. Wang, J. S. Liu, S. L. Chin, R. X. Li, and Z. Z. Xu, "Laser guided ionic wind," Sci. Rep. **8**, 13511 (2018).
16. G. Fibich and B. Ilan, "Multiple filamentation of circularly polarized beams," Phys. Rev. Lett. **89**, 013901 (2002).
17. S. Mitryukovskiy, Y. Liu, P. J. Ding, A. Houard, and A. Mysyrowicz, "Backward stimulated radiation from filaments in nitrogen gas and air pumped by circularly polarized 800 nm femtosecond laser pulses," Opt. Express **22**, 12750 (2014).
18. C. Meng, W. B. Chen, X. W. Wang, Z. H. Lu, Y. D. Huang, J. L. Liu, D. W. Zhang, Z. X. Zhao, and J. M. Yuan, "Enhancement of terahertz radiation by using circularly polarized two-color laser fields," Appl. Phys. Lett. **109**, 131105 (2016).
19. S. Rostami, M. Chini, K. Lim, J. P. Palastro, M. Durand, J. C. Diels, L. Arissian, M. Baudelet, and M. Richardson, "Dramatic enhancement of supercontinuum generation in elliptically-polarized laser filaments," Sci. Rep. **6**, 20363 (2016).
20. N. Chen, T.-J. Wang, Z. Zhu, H. Guo, Y. Liu, F. Yin, H. Sun, Y. Leng, and R. Li, "Laser ellipticity-dependent supercontinuum generation by femtosecond laser filamentation in air," Opt. Lett. **45**, 4444 (2020).
21. N. A. Panov, V. A. Makarov, V. Y. Fedorov, and O. G. Kosareva, "Filamentation of arbitrary polarized femtosecond laser pulses in case of high-order Kerr effect," Opt. Lett. **38**, 537 (2013).
22. N. A. Panov, O. G. Kosareva, A. B. Savel'ev, D. S. Uryupina, I. A. Perezhogin, and V. A. Makarov, "Filamentation of femtosecond Gaussian pulses with close-to-linear or -circular elliptical polarisation," Quantum Electron. **41**, 160 (2011).
23. M. Kolesik, J. V. Moloney, and E. M. Wright, "Polarization dynamics of femtosecond pulses propagating in air," Phys. Rev. E **64**, 046607 (2001).
24. Z. B. Zhu, T. J. Wang, Y. X. Liu, N. Chen, H. F. Zhang, H. Y. Sun, H. Guo, J. H. Zhang, X. Zhang, G. Y. Li, C. D. Liu, Z. N. Zeng, J. S. Liu, S. L. Chin, R. X. Li, and Z. Z. Xu, "Polarization-dependent femtosecond laser filamentation in air," Chin. Opt. Lett. **16**, 073201 (2018).

25. P. J. Ding, E. Oliva, A. Houard, A. Mysyrowicz, and Y. Liu, "Lasing dynamics of neutral nitrogen molecules in femtosecond filaments," Phys. Rev. A **94**, 043824 (2016).
26. S. Mitryukovskiy, Y. Liu, P. Ding, A. Houard, A. Couairon, and A. Mysyrowicz, "Plasma luminescence from femtosecond filaments in air: evidence for impact excitation with circularly polarized light pulses," Phys. Rev. Lett. **114**, 063003 (2015).
27. G. Ghosh, "Dispersion-equation coefficients for the refractive index and birefringence of calcite and quartz crystals," Opt. Commun. **163**, 95 (1999).
28. S. Petit, A. Talebpour, A. Proulx, and S. L. Chin, "Polarization dependence of the propagation of intense laser pulses in air," Opt. Commun. **175**, 323 (2000).
29. J. S. Liu, Z. L. Duan, Z. N. Zeng, X. H. Xie, Y. P. Deng, R. X. Li, Z. Z. Xu, and S. L. Chin, "Time-resolved investigation of low-density plasma channels produced by a kilohertz femtosecond laser in air," Phys. Rev. E **72**, 026412 (2005).
30. X. L. Liu, W. B. Cheng, M. Petrarca, and P. Polynkin, "Measurements of fluence profiles in femtosecond laser filaments in air," Opt. Lett. **41**, 4751 (2016).
31. S. I. Mitryukovskiy, Y. Liu, A. Houard, and A. Mysyrowicz, "Re-evaluation of the peak intensity inside a femtosecond laser filament in air," J. Phys. B: At. Mole. Opt. Phys. **48**, 094003 (2015).
32. H. Li, W. Chu, H. Zang, H. Xu, Y. Cheng, and S. L. Chin, "Critical power and clamping intensity inside a filament in a flame," Opt. Express **24**, 3424 (2016).
33. H. Guo, T.-J. Wang, X. Zhang, C. Liu, N. Chen, Y. Liu, H. Sun, B. Shen, Y. Jin, Y. Leng, and R. Li, "Direct measurement of radial fluence distribution inside a femtosecond laser filament core," Opt. Express **28**, 15529 (2020).
34. F. Theberge, W. W. Liu, P. T. Simard, A. Becker, and S. L. Chin, "Plasma density inside a femtosecond laser filament in air: strong dependence on external focusing," Phys. Rev. E **74**, 036406 (2006).
35. S. Akturk, A. Couairon, M. Franco, and A. Mysyrowicz, "Spectrogram representation of pulse self compression by filamentation," Opt. Express **16**, 17626 (2008).
36. A. Couairon, E. Brambilla, T. Corti, D. Majus, O. D. Ramirez-Gongora, and M. Kolesik, "Practitioner's guide to laser pulse propagation models and simulation," Eur. Phys. J. Spec. Top. **199**, 5 (2011).
37. N. Panov, V. Makarov, K. Grigoriev, M. Yatskevitch, and O. Kosareva, "Generation of polarization singularities in the self-focusing of an elliptically polarized laser beam in an isotropic Kerr medium," Phys. D: Nonlinear Phenom. **332**, 73 (2016).
38. J. P. Palastro, "Time-dependent polarization states of high-power, ultrashort laser pulses during atmospheric propagation," Phys. Rev. A **89**, 013804 (2014).
39. A. Couairon, S. Tzortzakis, L. Berge, M. Franco, B. Prade, and A. Mysyrowicz, "Infrared femtosecond light filaments in air: simulations and experiments," J. Opt. Soc. Am. B **19**, 1117 (2002).
40. A. Perelomov, V. Popov, and M. Terent'ev, "Ionization of atoms in an alternating electric field," Sov. Phys. JETP **23**, 207 (1967).
41. S. Popruzhenko, V. Mur, V. Popov, and D. Bauer, "Strong field ionization rate for arbitrary laser frequencies," Phys. Rev. Lett. **101**, 193003 (2008).
42. A. Bandrauk, E. Lorin, and J. V. Moloney, *Laser Filamentation: Mathematical Methods and Models* (Springer International, 2016), p. 112.
43. R. W. Boyd, *Nonlinear Optics* (Academic, 2020).